International Journal of Thermophysics, Vol. 14, No. 1, 1993

An Improved Parametric Crossover Model for the Thermodynamic Properties of Fluids in the Critical Region

S. B. Kiselev[1,2] and J. V. Sengers[2]

Received October 1, 1992

An improved parametric equation for the thermodynamic properties of fluids is presented that incorporates the crossover from singular thermodynamic behavior in the immediate vicinity of the critical point to regular thermodynamic behavior far away from the critical point. Based on a comparison with experimental data for ethane and methane, it is demonstrated that the crossover model is capable of representing the thermodynamic properties of fluids in a large range of temperatures and densities around the critical point.

KEY WORDS: critical phenomena; equation of state; ethane; methane; sound velocity; specific heat; thermodynamic properties.

1. INTRODUCTION

A characteristic feature of thermodynamic states of a fluid in the vicinity of the vapor–liquid critical point is the presence of long-range fluctuations in the density. The intensity of these fluctuations diverges at the critical point. As a consequence, the thermodynamic surface of fluids exhibits a singularity at the critical point. The asymptotic singular critical behavior of the thermodynamic properties can be described in terms of scaling laws with universal exponents and universal scaling functions [1, 2]. In order to obtain an equation of state for fluids in the immediate vicinity of the critical point, one commonly introduces two parametric variables, r and ϑ,

[1] Institute for Oil and Gas Research of the Russian Academy of Sciences, Leninsky Prospect 65, Moscow 117917, Russia.

[2] Institute for Physical Science and Technology, University of Maryland, College Park, Maryland 20742, U.S.A.

840/14/1-1

such that r measures a distance from the critical point [1–4]. By incorporating the critical singularities as power laws in terms of the variable r, while the ϑ dependence is kept analytic, one avoids any spurious singularities in the one-phase region away from the critical point [3] and can formulate an equation of state that is fully consistent with the theoretical predictions for the critical-point singularity. A scaled parametric equation most commonly adopted is the so-called linear model originally introduced by Schofield et al. [5].

Fluids near the critical point satisfy the same asymptotic scaling laws as symmetric three-dimensional Ising-like systems [1, 2]. However, a serious problem is that these asymptotic scaling laws are valid only in an extremely small range of temperatures and densities around the critical point [6]. Attempts have been made to extend the asymptotic linear-model equation of state by including a confluent singularity and by incorporating a revision that accounts for lack of vapor–liquid symmetry [7–10]. These more general parametric equations of state have been used to represent the thermodynamic properties of many fluids near the critical point [1, 4, 8–13]. Nevertheless, the range of these equations of state is still sufficiently restricted so that they have not yet received wide acceptance for practical applications in the engineering literature [14].

On the other hand, it has become evident that critical fluctuations are actually present in fluids in a very large range of temperatures and densities [15, 16]. Hence, to account for the effects of these critical fluctuations on the equation of state, it is necessary to consider also the nonasymptotic critical behavior of the thermodynamic properties including the crossover to regular classical behavior far away from the critical point.

A parametric model that incorporates crossover from singular behavior near the critical point to regular behavior far away from the critical point has recently been developed by Luettmer-Strathmann et al. [17]. This parametric model is based on a theory of nonasymptotic critical behavior initiated by Nicoll and co-workers [18, 19] and further developed by Chen and co-workers [15, 20]. The theoretical approach starts from a classical Landau expansion, which is renormalized to account for the critical fluctuations.

A phenomenological attempt to formulate a parametric model that also accounts for the crossover to regular behavior far away from the critical point has been made by Kiselev and co-workers [4, 21, 22]. We have continued a study, initiated by Anisimov et al. [16], comparing this phenomenological crossover model with the theoretical results for the crossover behavior mentioned above. This study has led us to introduce some modifications into the earlier crossover model of Kiselev et al. In this paper we show that the improved phenomenological parametric crossover

model not only is capable of representing the thermodynamic properties of fluids at temperatures up to temperatures as high as twice the critical temperature, but also accounts for the thermodynamic properties in the two-phase region in a substantial range of temperatures below the critical temperature.

We proceed as follows. In Section 2, we review the known asymptotic scaling-law behavior of the thermodynamic properties as well as some previous attempts to include correction terms to account for the lack of vapor–liquid symmetry and for the presence of a confluent singularity. In Section 3, we summarize some issues related to the expected crossover behavior of the Helmholtz free energy. In Section 4 we formulate a phenomenological parametric crossover model for the Helmholtz free energy. This crossover model is a modification of a phenomenological crossover model earlier proposed by Kiselev et al. [4, 21, 22]. This model is compared with experimental thermodynamic-property data in Section 5. Our results are summarized in Section 6.

2. ASYMPTOTIC SCALING-LAW BEHAVIOR

Let V be the volume, ρ the density, T the temperature, μ the chemical potential, $\chi = (\partial\rho/\partial\mu)_T$ a susceptibility, A the Helmholtz free energy and C_v the heat capacity at constant volume. These thermodynamic quantities are made dimensionless with the aid of the critical temperature T_c, critical density ρ_c, and critical pressure P_c [1]

$$\left.\begin{aligned} &\tilde{T} = -T_c/T, && \tilde{\rho} = \rho/\rho_c, && \tilde{\mu} = \mu\rho_c T_c/P_c T \\ &\tilde{\chi} = \chi P_c T/\rho_c^2 T_c, && \tilde{A} = AT_c/VP_c T, && \tilde{c}_v = C_v T_c/VP_c \end{aligned}\right\} \tag{1}$$

In addition, we define

$$\tau = \tilde{T} + 1 = (T - T_c)/T, \qquad \Delta\rho = \tilde{\rho} - 1 \tag{2}$$

$$\Delta\tilde{\mu} = \tilde{\mu} - \tilde{\mu}_0(T) \tag{3}$$

$$\Delta\tilde{A} = \tilde{A} - \tilde{\rho}\tilde{\mu}_0(T) - \tilde{A}_0(T) \tag{4}$$

where $\tilde{\mu}_0(T)$ and $\tilde{A}_0(T)$ are analytic functions of temperature such that $\Delta\tilde{\mu} = 0$ and $\tilde{A}_0 = -1$ at the critical point. The idea is that $\Delta\tilde{A}$ incorporates the effect of the critical fluctuations, while the functions $\tilde{\mu}_0(T)$ and $\tilde{A}_0(T)$ are in practice represented by truncated Taylor expansions of the form [15, 17]

$$\tilde{\mu}_0(T) = \sum_{j=0} \mu_j \tau^j, \qquad \tilde{A}_0(T) = -1 + \sum_{j=1} A_j \tau^j \tag{5}$$

According to the theory of critical phenomena, the Helmholtz free-energy density A/V satisfies close to the critical point a scaling law of the form [1, 2]

$$\Delta\tilde{A} = |u_\tau|^{2-\alpha}[f_0(u_h/|u_\tau|^{\beta\delta}) \tag{6}$$

where the scaling fields u_τ and u_h are asymptotically proportional to τ and $\Delta\tilde{\mu}$, respectively, while α, β, and δ are critical exponents. In fact, Eq. (6) is the first term of a so-called Wegner expansion [23, 24]

$$\Delta\tilde{A} = |u_\tau|^{2-\alpha}\left[f_0(u_h/|u_\tau|^{\beta\delta}) + \sum_{i=1}^{n} c_i|u_\tau|^{\Delta_i} f_i(u_h/|u_\tau|^{\beta\delta})\right] \tag{7}$$

where, more generally, u_τ and u_h are analytic functions of τ and $\Delta\mu$, while c_i are additional system-dependent coefficients. As a consequence, various thermodynamic properties exhibit power-law behavior when the critical point is approached along the critical isochore ($\Delta\rho = 0$), along the critical isotherm ($\tau = 0$) or along the coexistence curve ($\Delta\rho = \Delta\rho_{\text{cxc}}$). The first two terms of these power-law expansions for a number of properties are listed in Table I. The critical exponents are related by

$$2 - \alpha = \beta(\delta + 1), \qquad \gamma = 2 - \alpha - 2\beta \tag{8}$$

The critical exponents, as well as the scaling functions f_i in Eq. (7), are universal. Fluids belong to the universality class of three-dimensional Ising-like systems with exponent values [1, 4, 25]

$$\alpha = 0.11, \qquad \beta = 0.325, \qquad \Delta_1 = 0.51 \tag{9}$$

Universality of the scaling function f_0 in Eqs. (6) and (7) implies that only two of the amplitudes A^+, A^-, Γ^+, Γ^-, D, and B can be treated as system-dependent constants. Similarly, universality of the scaling function

Table I. Critical Power-Law Expansions

Property	Power-law expansions	Path
$\tilde{c}_V = -\tilde{T}^2(\partial^2\tilde{A}/\partial\tilde{T}^2)_\rho$	$A^+\tau^{-\alpha}(1 + A_1^+\tau^{\Delta_1} + \cdots)$	$\Delta\rho = 0, \tau \geqslant 0$
$\tilde{c}_V = -\tilde{T}^2(\partial^2\tilde{A}/\partial\tilde{T}^2)_\rho$	$A^-\lvert\tau\rvert^{-\alpha}(1 + A_1^-\lvert\tau\rvert^{\Delta_1} + \cdots)$	$\Delta\rho = 0, \tau \leqslant 0$
$\tilde{\chi} = (\partial\tilde{\rho}/\partial\tilde{\mu})_T$	$\Gamma^+\tau^{-\gamma}(1 + \Gamma_1^+\tau^{\Delta_1} + \cdots)$	$\Delta\rho = 0, \tau \geqslant 0$
$\tilde{\chi} = (\partial\tilde{\rho}/\partial\tilde{\mu})_T$	$\Gamma^-\lvert\tau\rvert^{-\gamma}(1 + \Gamma_1^-\lvert\tau\rvert^{\Delta_1} + \cdots)$	$\Delta\rho = \Delta\rho_{\text{cxc}}, \tau \leqslant 0$
$\Delta\tilde{\mu} = (\partial\Delta\tilde{A}/\partial\Delta\rho)_T$	$\pm D\lvert\Delta\rho\rvert^{\delta}(1 + D_1\lvert\Delta\rho\rvert^{\Delta_1/\beta} + \cdots)$	$\tau = 0$
$\lvert\Delta\rho_{\text{cxc}}\rvert$	$B\lvert\tau\rvert^{\beta}(1 + B_1\lvert\tau\rvert^{\Delta_1} + \cdots)$	$\tau \leqslant 0$

f_1 in Eq. (7) implies that only one of the correction-to-scaling amplitudes A_1^+, A_1^-, Γ_2^+, Γ_1^-, D_1, and B_1 can be treated as a system-dependent constant.

In order to formulate an equation of state based on the asymptotic scaling-law behavior in Eq. (6), one introduces two parametric variables r and ϑ. There are several ways in which this can be done, but the parametric equations most commonly adopted are [3, 4]

$$\tau = r(1 - b^2\vartheta^2) \tag{10}$$

$$\Delta\rho = kr^\beta\vartheta \tag{11}$$

$$\Delta\tilde{\mu} = ar^{\beta\delta}\vartheta(1 - \vartheta^2) \tag{12}$$

where a and k are the two system-dependent constants that enter into the asymptotic scaling-law behavior, while b^2 is a universal constant. In the original formulation, Eqs. (10) and (12) defined the transformation, while $\Delta\rho$ was then assumed to be linear in ϑ [5]. In practice, though, we use Eqs. (10) and (11) to convert the physical variables τ and $\Delta\rho$ into the parametric variables r and ϑ.

The relationships between the amplitudes of the asymptotic critical power laws and the linear-model constants a, k, and b^2 are presented in Table II. The universal constant b^2 is selected so as to obtain agreement with the known theoretical values of the universal relations among the amplitudes of the asymptotic critical power laws. A possible choice is

$$b^2 = (\gamma - 2\beta)/\gamma(1 - 2\beta) = 1.359 \tag{13}$$

which corresponds to the so-called restricted linear model [3–5]. With this value of b^2 we obtain

$$A^+/A^- = 0.52, \quad \Gamma^+/\Gamma^- = 4.87, \quad A^*\Gamma^+/B^2 = 0.056, \quad \Gamma^+ DB^{\delta-1} = 1.69 \tag{14}$$

Table II. Amplitudes of Critical Power Laws

Asymptotic critical amplitudes	
$A^+ = ak\gamma(\gamma-1)/2\alpha b^2$	$\Gamma^+ = k/a$
$D = a(b/k)^\delta(b^2-1)/b$	$B = k/(b^2-1)^\beta$
$A^-/A^+ = [(1-2\beta)/(\gamma-1)]^2(b^2-1)^\alpha$	$\Gamma^-/\Gamma^+ = (1-2\beta)(b^2-1)/2(\gamma-1)$
$D\Gamma^+B^{\delta-1} = b^{\delta-3}(b^2-1)^{\gamma-1}$	$A^+\Gamma^+B^2 = \gamma(\gamma-1)(b^2-1)^{2\beta}/2\alpha b^2$

Correction-to-scaling amplitudes

$$A_1^+ = \Gamma_1^+(\gamma + \Delta_1)\alpha/\gamma(\gamma-1), \qquad \Gamma_1^+ = -c_1/a, \qquad B_1 = \Gamma_1^+/2(b^2-1)^{\beta+\Delta_1}$$

in good agreement with the theoretical values as reviewed by Tang et al. [26].

The linear-model equations imply for the Helmholtz free-energy density

$$\Delta\tilde{A} = akr^{2-\alpha}\Psi_0(\vartheta) \tag{15}$$

where the function $\Psi_0(\vartheta)$ is given in Table III. It turns out that the asymptotic scaling-law behavior applies only in an extremely small range around the critical point [6]. To represent actual thermodynamic-property data in the critical region, it is necessary to revise the asymptotic scaling-law behavior to account for lack of vapor-liquid symmetry and to extend it by including the first correction term in the Wegner expansion given by Eq. (7). Two revised and extended scaled parametric equations of state have been widely used for this purpose, namely, one proposed by Balfour et al. [7] and one proposed by Kiselev [9]. Here we consider the latter version.

It is first noted that a more appropriate order parameter for a fluid near the critical point is not $\Delta\rho$ itself, but

$$m = \Delta\rho - d_1\tau \tag{16}$$

where d_1 is a system-dependent constant related to the diameter of the coexistence curve [4, 15]. Furthermore, the scaling fields u_τ and u_h in Eq. (6) are not simply proportional to τ and $\Delta\tilde{\mu}$, but should be taken as linear combinations of τ and $\Delta\tilde{\mu}$, a procedure often referred to as mixing of the scaling fields. Finally, the leading correction terms in the Wegner expansion given by Eq. (7) must be incorporated. A revised and extended parametric model accounting for these effects can be defined by the following set of equations [9, 10]:

$$\tau = r(1 - b^2\vartheta^2) \tag{17}$$

$$m = \Delta\rho - d_1\tau = kr^\beta\vartheta \tag{18}$$

$$\Delta\tilde{A} = kr^{2-\alpha}\left[a\Psi_0(\vartheta) + \sum_{i=1}^{5} c_i r^{\Delta_i}\Psi_i(\vartheta)\right] \tag{19}$$

Table III. The Functions $\Psi_i(\vartheta)$ in the Parametric Model

$$\Psi_0(\vartheta) = (1/2b^4)[2\beta(b^2-1)/(2-\alpha) + 2\beta(2\gamma-1)(1-b^2\vartheta^2)/\gamma(1-\alpha) + (2\beta-1)(1-b^2\vartheta^2)^2/\alpha]$$
$$\Psi_1(\vartheta) = [1/2b^2(1-\alpha+\Delta_1)][(\gamma+\Delta_1)/(2-\alpha+\Delta_1) - (1-2\beta)b^2\vartheta^2]$$
$$\Psi_2(\vartheta) = [1/2b^2(1-\alpha+\Delta_2)][(\gamma+\Delta_2)/(2-\alpha+\Delta_2) - (1-2\beta)b^2\vartheta^2]$$
$$\Psi_3(\vartheta) = \vartheta - (2/3)(e-\beta)b^2\vartheta^3 + (1-2\beta)e_1b^4\vartheta^5/(5-2e)$$
$$\Psi_4(\vartheta) = (1/3)b^2\vartheta^3 + (1-2\beta)e_2b^4\vartheta^5/(5-2e)$$
$$\Psi_5(\vartheta) = (1/3)b^2\vartheta^3 + (1-2\beta)e_4b^4\vartheta^5/(5-2e_3)$$

with

$$\Delta_2 = 2\Delta_1, \qquad \Delta_3 = \Delta_4 = \gamma + \beta - 1 \tag{20}$$

while Δ_5 is the exponent of the asymmetric correction term in the Wegner expansion, sometimes also designated as Δ_a [15, 17, 25]. The explicit expressions for the functions $\Psi_i(\vartheta)$ in Eq. (19) are presented in Table III. The functions Ψ_0, Ψ_1, Ψ_3, and Ψ_4 are identical with the functions designated Ψ_a, Ψ_c, Ψ_d, and Ψ_f in previous publications [9, 10, 13]. It should be noted that the terms for $i=2$ and $i=5$ were not included in the previous work of Kiselev and co-workers but have been included here for use in formulating our parametric crossover model in Section 4. The terms with exponents Δ_1, Δ_2, and Δ_5 in Eq. (19) represent correction terms that appear in the Wegner expansion. However, the terms with Δ_3 and Δ_4 in Eq. (19) do not correspond to any terms in the Wegner expansion but originate from the mixing of the scaling fields in the expressions for the asymptotic scaling law given by Eq. (6) [9, 10]. With $c_2 = c_5 = 0$, the revised and extended linear model defined by Eqs. (17)–(19) has been used to represent the thermodynamic properties of number of fluids in the critical region [10, 13, 27]. For the ratios of the correction-to-scaling amplitudes, this model implies $A_1^+/\Gamma_1^+ = 0.65$ and $B_1/\Gamma_1^+ = 0.84$ to be compared with the theoretical values $A_1^+/\Gamma_1^+ = 0.95 \pm 0.03$ and $B_1/\Gamma_1^+ = 0.9 \pm 0.2$ [26].

An alternative revised and extended parametric model, originally proposed by Balfour et al. [7], has been used extensively by Sengers and co-workers [1, 8, 11, 12]. The primary difference is that in the latter version the mixing of the scaling field is represented by one system-dependent parameter c, while in Eq. (19) two system-dependent constants c_3 and c_4 account for this mixing. A comparative study of the two revised and extended parametric equations of the state has been made by Aizpiri et al. [14].

The range of applicability of either version is still limited and corresponds roughly to $\tau \leqslant 0.06$ and $|\Delta\rho| \leqslant 0.3$ in the one-phase region, while the temperature range in the two-phase region is more restricted [1]. On the other hand, the effect of critical fluctuations on the equation of state can be neglected only when τ is much larger than the so-called Ginzburg number *Gi*. This criterion suggests that critical fluctuations may be present even at temperatures twice the critical temperature [16]. Hence, to account fully for the effect of the critical fluctuations an asymptotic analysis is inadequate and a more complete account of the nonasymptotic effects of the critical fluctuations, including the crossover of the equation of state to regular behavior far away from the critical point, must be incorporated.

3. THEORY OF THERMODYNAMIC CROSSOVER BEHAVIOR

A theoretical approach for constructing a Helmholtz free-energy density that incorporates crossover from singular behavior asymptotically close to the critical point to regular behavior far away from the critical point has been developed by Chen et al. [15] based on earlier work of Nicoll co-workers [18–20]. In this approach one starts from the observation that in the classical theory of critical phenomena, $\Delta\tilde{A}$ can be expanded in a Landau expansion of the form [15]

$$\Delta\tilde{A}_{\rm cl} = (1/2)tM^2 + (1/4!)\,u\Lambda M^4 + (1/5!)\,a_{05}M^5 + (1/6!)\,a_{06}M^6 + (1/4!)\,a_{14}tM^4 + (1/2!2!)\,a_{22}t^2M^2\cdots \tag{21}$$

where the Landau variables t and M are related to the physical variables τ and m through two scale factors, c_t and c_ρ,

$$t = c_t\tau, \qquad M = c_\rho m = c_\rho(\Delta\rho - d_1\tau) \tag{22}$$

The two system-dependent constants c_t and c_ρ play the role of two system-dependent amplitudes in the asymptotic universal scaling-law behavior. The coefficients in the Landau expansion given by Eq. (21) are all system-dependent constants; the coefficient of the M^4 term has been written as a product of a coupling constant u and a parameter Λ that is related to the maximum cutoff wave number of the critical fluctuations [18–20]. It is then argued that the critical fluctuations renormalize the critical expansion into [15, 20]

$$\Delta\tilde{A}_{\rm r} = (1/2)\,tM^2\mathscr{T}\mathscr{D} + (1/4!)\,u^*\bar{u}\Lambda M^4\mathscr{D}^2\mathscr{U} + (1/5!)\,a_{05}M^5\mathscr{D}^{5/2}\mathscr{V}\mathscr{U} + (1/6!)\,a_{06}M^6\mathscr{D}^3\mathscr{U}^{3/2} + (1/4!)\,a_{14}tM^4\mathscr{T}\mathscr{D}^2\mathscr{U}^{1/2} + (1/2!2!)\,a_{22}t^2M^2\mathscr{T}^2\mathscr{D}\mathscr{U}^{-1/2} - (1/2)\,t^2\mathscr{K} \tag{23}$$

where $\mathscr{T}$, $\mathscr{D}$, $\mathscr{U}$, $\mathscr{V}$, and $\mathscr{K}$ are rescaling functions related to a crossover function Y by

$$\left.\begin{aligned} \mathscr{T} &= Y^{(2\nu-1)/\Delta_1}, & \mathscr{D} &= Y^{(\gamma-2\nu)/\Delta_1}, & \mathscr{U} &= Y^{\nu/\Delta_1} \\ \mathscr{V} &= Y^{(2\Delta_5-\nu)/2\Delta_1}, & \mathscr{K} &= (\nu/\alpha\bar{u}\Lambda)(Y^{-\alpha/\Delta_1}-1) \end{aligned}\right\} \tag{24}$$

Here $\nu = \beta(\delta+1)/3$ is the critical exponent for the asymptotic critical power law of the correlation length ξ [1], while

$$\bar{u} = u/u^* \tag{25}$$

where $u^* = 0.472$ is a universal coupling constant [20]. Far away from the critical point the crossover function Y approaches unity and Eq. (23) reduces to the classical Landau expansion given by Eq. (21). We note that the first term asymmetric in the order parameter M in this Landau expansion is proportional to M^5. The reason is that the other asymmetric terms proportional to M, t^2M, and M^3 are accounted for by a mixing transformation of the form [15, 20]

$$\Delta\tilde{A} = \Delta\tilde{A}_r - c(\partial\Delta\tilde{A}_r/\partial M)_t(\partial\Delta\tilde{A}_r/\partial t)_M \tag{26}$$

with

$$t = c_t\tau + c(\partial\Delta\tilde{A}_r/\partial M)_t, \qquad M = c_\rho(\Delta\rho - d_1\tau) + c(\partial\Delta\tilde{A}_r/\partial t)_M \tag{27}$$

where the coefficient c determines the strength of mixing. We again note that in this approach the strength of the mixing is represented by one system-dependent coefficient c, while in Eq. (19) for $\Delta\tilde{A}$ this mixing is represented by two coefficients c_3 and c_4.

Possible closed-form approximants for the crossover function Y have been discussed by Tang et al. [26]. The simplest form is

$$Y = \{1 + \bar{u}[(1 + \Lambda^2/\kappa^2)^{\Delta_1/2\nu} - 1]\}^{-1} \tag{28}$$

with

$$\kappa^2 = t\mathscr{T} + (1/2)\, u^*\Lambda M^2\mathscr{D}\mathscr{U} \tag{29}$$

referred to as crossover model I by Tang et al. [26]. As shown by Luettmer-Strathmann et al. [17], this theoretical crossover model (with some slightly modified expressions for $\mathscr{U}$ and $\mathscr{K}$) can be expressed in terms of parametric variables $\tilde{r}$ and ϕ, such that

$$t = \tilde{r}Z^{-(2-1/\nu)/\omega}(1 - \phi^2/2) \tag{30}$$

$$M = (u^*\bar{u}\Lambda)^{-1/2}(\tilde{r}^{2\nu} + \Lambda^2)^{(1-\omega)/4}\tilde{r}^{\beta}Z^{(\eta-\omega)/2\omega}\phi \tag{31}$$

$$\Delta\tilde{A}_r = \sum_{i=1}^{7} \tilde{c}_i F_i(\phi)\, f_i(\tilde{r}) \tag{32}$$

with

$$\eta = 2 - \gamma/\nu, \qquad \omega = \Delta_1/\nu \tag{33}$$

and where

$$Z(\tilde{r}) = [(1 - \bar{u})\tilde{r}^{\omega\nu} + \bar{u}(\tilde{r}^{2\nu} + \Lambda^2)^{\omega/2}]^{-1} \tag{34}$$

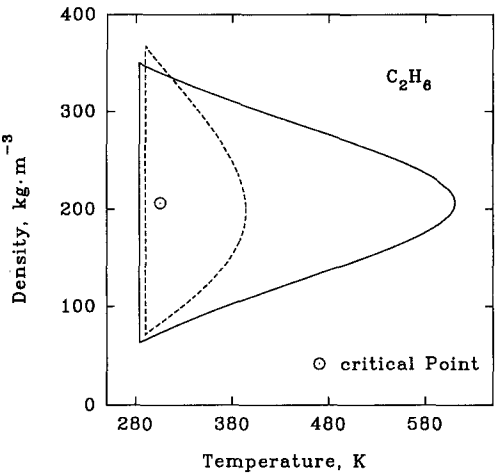

Fig. 1. Range of improved crossover model for ethane corresponds to area inside solid curve. Range of crossover model as previously implemented by Luettmer-Strathmann et al. [17] corresponds to area inside dashed curve.

The explicit expressions for the coefficients $\tilde{c}_i$ and the functions $F_i(\phi)$ and $f_i(\tilde{r})$ are given in the paper by Luettmer-Strathmann et al. [17]. Near the critical point Eqs. (30) and (31) indeed reduce to the linear-model equations, Eqs. (10) and (11), but Eq. (32) for $\Delta\tilde{A}_r$ remains slightly different from the linear-model expression, Eq. (13). However, it should be noted that the linear model is correct only in a perturbation expansion up to second order in $\varepsilon = 4 - d$ [28, 29], where d is the dimensionality. Hence, the existence of a small difference with a comprehensive estimate of the effects of the critical fluctuations on the equation of state can be expected.

As demonstrated in previous publications [15, 17], this crossover model, based on a six-term renormalized Landau expansion, represents the thermodynamic properties in a range of temperature and density approximately bounded by $\tilde{\chi}^- \leqslant 2.2$. For example, in the case of ethane this range corresponds to the region inside the dashed curve shown in Fig. 1.

4. PHENOMENOLOGICAL CROSSOVER MODEL

A phenomenological procedure for dealing with the crossover behavior of the Helmholtz free energy density has been proposed by Kiselev et al. [21, 22]. In this approach one starts from the revised and

extended parametric equation, Eq. (19), for $\Delta\tilde{A}$ and modifies each term so that they all become analytic far away from the critical point, i.e., for large values of the variable r. For this purpose we use a crossover function $R(q)$ defined by

$$R(q) = 1 + q^2/(q_0 + q) \tag{35}$$

where q_0 is a universal constant, initially taken to be unity [21], and subsequently modified to $q_0 = 0.3$ [22], while the variable q is related to the parametric variable r by

$$q = rg \tag{36}$$

An expression for $\Delta\tilde{A}$ that reduces to Eq. (19) for $q \to 0$ $(r \ll g^{-1})$ and becomes analytic for $q \to \infty$ $(r \gg g^{-1})$ is then obtained by the set of equations

$$\tau = r(1 - b^2\vartheta^2) \tag{37}$$

$$m = \Delta\rho - d_1\tau = kR^{-\beta+1/2}(q) r^\beta \vartheta \tag{38}$$

$$\Delta\tilde{A} = kr^{2-\alpha} R^\alpha(q) \left[a\Psi_0(\vartheta) + \sum_{i=1}^{5} c_i r^{\Delta_i} R^{-\Delta_i}(q)\, \Psi_i(\vartheta) \right] \tag{39}$$

As demonstrated in previous publications [16, 21], the system-dependent coefficient g in the relationship between q and r is proportional to the inverse of the Ginzburg number Gi.

The phenomenological crossover model, as defined by Eqs. (37)–(39), differs from the crossover model previously employed by Kiselev et al. [21, 22] in the following aspects. First, we have added the terms $i = 2$ and 3 with critical exponents $\Delta_2 = 2\Delta_1$ and Δ_5, which were absent in the previous formulation. Second, we have replaced the variable $(T - T_c)/T_c$ by the modified variable $\tau = (T - T_c)/T$, as done in the work of Chen et al. [15, 20]. Theoretical arguments that $1/T$ is the more appropriate variable have been presented in the literature [24, 30, 31]. As we shall see in the next section the phenomenological crossover model with these modifications is capable of representing thermodynamic-property data of fluids in a significantly larger range of temperatures and densities around the critical point than any crossover model proposed previously.

Our phenomenological crossover model is specified by Eqs. (37)–(39), summarized explicitly in Appendix I, together with Eqs. (4) and (5). It contains the following universal constants: the critical exponents, the linear-model parameter b^2 as given by Eq. (13), and the crossover constant $q_0 = 0.3$. For the critical exponents α, β, and Δ_1 we adopt the values given

Table IV. Universal Critical-Region Constants

$\alpha = 0.11, \quad \beta = 0.325$	$\Delta_1 = 0.51, \quad \Delta_5 = 1.19$
$q_0 = 0.3, \quad A_0 = -1$	$\Delta_2 = 2\Delta_1, \quad \Delta_3 = \Delta_4 = \gamma + \beta - 1$
$\gamma = 2 - \alpha - 2\beta$	$\delta = (2 - \alpha - \beta)/\beta$
$b^2 = (\gamma - 2\beta)/\gamma(1 - 2\beta)$	$e = 2\gamma + 3\beta - 1$
$e_1 = (5 - 2e)(e - \beta)(3 - 2e)/3(5\beta - e)$	$e_2 = (5 - 2e)(e - 3\beta)/3(5\beta - e)$
$e_3 = 2 - \alpha + \Delta_5$	$e_4 = (5 - 2e_3)(e_3 - 3\beta)/3(5\beta - e_3)$

by Eq. (9). The value of the critical exponent Δ_5 is not well-known [18, 24, 32, 33]; we have adopted the value 1.19 recommended by Zhang [34]. The values of all universal constants for the phenomenological crossover model are listed in Table IV.

It is of interest to compare this phenomenological crossover model with the theoretical crossover model discussed in Section 3, which is based on a renormalized Landau expansion. For this purpose it is illustrative to introduce a function $\tilde{Y}(q)$ defined by

$$\tilde{Y}(q) = [q/R(q)]^{\Delta_1} \tag{40}$$

As shown in Appendix II, the parametric expression (39) for $\Delta\tilde{A}$ can then be transformed into

$$\begin{aligned} \Delta\tilde{A} = {} & (1/2)\,\hat{a}_{12}\tau M^2 \mathscr{T}\mathscr{D} + (1/4!)\,\hat{a}_{04} M^4 \mathscr{D}^2 \mathscr{U} + (1/5!)\,\hat{a}_{05} M^5 \mathscr{D}^{5/2} \mathscr{V} \mathscr{U} \\ & + (1/3!)\,\hat{a}_{13}\tau M^3 \mathscr{T}\mathscr{D}^{3/2}\mathscr{V} + (1/2)\,\hat{a}_{21}\tau^2 M \mathscr{T}^2 \mathscr{D}^{1/2} \mathscr{V}_1 \mathscr{U}^{-1} \\ & - (1/2)\,\hat{a}_0 \tau^2 \mathscr{K} - (1/2)\,\hat{a}_0 \tau^2 \end{aligned} \tag{41}$$

with coefficients $\hat{a}_0$ and $\hat{a}_{ij}$ also specified in Appendix II. The interesting point is that the functions $\mathscr{T}$, $\mathscr{D}$, $\mathscr{U}$, $\mathscr{V}$, and $\mathscr{K}$ are identical to the rescaling functions of Chen et al. [15] as given by Eq. (24), with the crossover function Y replaced $\tilde{Y}$. In addition, one new rescaling function, $\mathscr{V}_1$, appears, which is defined by

$$\mathscr{V}_1 = \tilde{Y}^{(2\Delta_3 - \nu)/\Delta_1} \tag{42}$$

On comparing Eqs. (23) and (41) we see a similar structure, but there are some differences. The first difference is that, unlike the coefficients a_{ij} in the expansion given by Eq. (23), the coefficients $\hat{a}_{ij}$ in Eq. (41) also depend on the crossover function $\tilde{Y}$. This is related to the fact that we have imposed the condition that Eq. (41) should reduce to the linear-model expression, Eq. (13), while the theoretical crossover model given by Eq. (23) does not precisely recover the linear model as mentioned in Section 3. We also do not have terms proportional to τM^4, $\tau^2 M^2$ and M^6. The second difference

is that Eq. (41) contains asymmetric terms proportional to τM^3 and $\tau^2 M$ that are absent in the Landau expansion given by Eq. (21) and, hence, in Eq. (23). The reason is that in the crossover theory of Chen et al. [15, 20] these asymmetry effects are handled by the mixing transformation given by Eqs. (26) and (27), while in the phenomenological crossover model these asymmetry terms are entered directly. The third difference is the appearance of a term proportional to τ^2, which modifies the analytic background $\tilde{A}_0(T)$ given by Eq. (5). Apart from the way in which the mixing of the scaling fields is treated, the two expansions, Eqs. (23) and (41), are rather similar. In fact it turns out that the effectiveness of either crossover model is determined largely by the choice of the crossover function Y or $\tilde{Y}$. New results obtained by Jin et al. [35] for the theoretical crossover model confirm this conclusion.

5. COMPARISON WITH EXPERIMENTAL DATA

For a comparison of our extended phenomenological crossover model with experimental data, we consider here the thermodynamic properties of ethane and methane earlier analyzed by Luettmer-Strathmann [17] and co-workers and by Jin et al. [36] in terms of the renormalized Landau expansion discussed in Section 3. As in these previous papers, all temperatures refer to the new international temperature scale of 1990 (ITS-90) [37].

The phenomenological crossover model, defined by Eqs. (35)–(39) together with Eqs. (4) and (5), contains the following system-dependent constants: the critical parameters T_c, ρ_c, and P_c, the rescaled asymptotic critical amplitude k of the coexistence curve, the linear-diameter amplitude d_1 of the coexistence curve, the amplitude a of the asymptotic and amplitudes c_i ($i = 2$–5) of the nonasymptotic terms in the parametric representation, the inverse rescaled Ginzburg number g, and also the coefficients A_i in the background contribution to the pressure and the coefficients μ_i in the background contribution to the caloric properties. The values of these system-dependent constants for ethane and methane are presented in Table V.

For ethane we adopt the values of the critical parameters reported by Douslin and Harrison [38], with T_c changed to ITS-90,

$$T_c = 305.322 \text{ K}, \qquad P_c = 4.8718 \text{ MPa}, \qquad \rho_c = 206.581 \text{ kg} \cdot \text{m}^{-3} \quad (43)$$

as adopted earlier also by Luettmer-Strathmann et al. [17]. For methane we adopt the same critical parameters as used by Jin et al. [36]:

$$T_c = 190.564 \text{ K}, \qquad P_c = 4.5992 \text{ MPa}, \qquad \rho_c = 162.380 \text{ kg} \cdot \text{m}^{-3} \quad (44)$$

Table V. System-Dependent Constants in the Crossover Model for Ethane and Methane

	Ethane	Methane
Critical parameters		
T_c (K)	305.322	190.564
P_c (MPa)	4.8718	4.5992
ρ_c (kg · m^{-3})	206.581	162.380
Critical coefficients		
k	1.1276	1.0498
d_1	−0.6046	−0.4889
a	18.525	16.426
c_1	−8.9866	−11.066
c_2	13.311	19.998
c_3	−5.6546	−3.7608
c_4	5.9308	3.6660
c_5	−0.7666	−0.5386
Inverse Ginzburg number		
g	1.1599	2.0066
Background coefficients		
A_1	−5.4681	−4.9847
A_2	15.606	13.171
A_3	−0.4667	0.1925
A_4	1.6179	0.2692
μ_2	−13.212	−8.1067
μ_3	−3.2387	−4.6087
μ_4	−26.795	3.2184
μ_5		−14.837

These values of T_c and P_c for methane are identical to the values obtained by Kleinrahm and Wagner [39], but the critical density $\rho_c = 162.380\ \text{kg} \cdot \text{m}^{-3}$ is slightly lower than the value $\rho_c = 162.660\ \text{kg} \cdot \text{m}^{-3}$ reported by Kleinrahm and Wagner. This small difference is related to the presence of an asymptotic singular behavior of the coexistence curve predicted by the scaling laws [24].

Except for the caloric background coefficients μ_i, all other system-dependent constants have been determined from a fit of the crossover model to the experimental P–ρ–T data obtained by Douslin and Harrison [38] for ethane and to the experimental P–ρ–T data obtained by Wagner and co-workers [40, 41] and by Trappeniers et al. [42] for methane. With estimated errors in pressure, temperature, and density as small as $\sigma_P = 0.00005$ MPa, $\sigma_T = 0.001$ K, and $\sigma_\rho = 0.15\ \text{kg} \cdot \text{m}^{-3}$ [17, 36], we find that the equation represents the experimental pressure data with a reduced

chi-square of 3.7 for ethane and of 3.6 for methane in a range of temperatures and densities bounded by

$$\tau + 1.2\Delta\rho^2 \leqslant 0.5 \qquad \text{and} \qquad T \geqslant T_m \tag{45}$$

where $T_m = 284$ K for ethane and $T_m = 178$ K for methane. This range is shown in Fig. 1 for ethane and in Fig. 2 for methane. Percentage deviations of the experimental pressures from the calculated pressures are shown in Fig. 3 for ethane and in Fig. 4 for methane. These percentage deviations are less then 0.15% inside the region specified by Eq. (45) and increase up to 0.25–0.35% at the boundary. These pressure deviations are not as small as those found by Luettmer-Strathmann et al. [17] for ethane and by Jin et al. [36] for methane, but the present crossover model covers a significantly larger temperature range, as shown in Figs. 1 and 2. The pressure deviations are also not as small as those corresponding to the empirical multiparameter analytic global equation developed by Setzmann and Wagner [43] for methane, but the crossover model yields a significantly better representation of the caloric properties near the critical point as shown below.

The coefficients μ_0 and μ_1 in Eq. (5) determine the zero points of entropy and internal energy and are not considered here. The coefficients μ_i for $i \geqslant 2$ determine the backround contributions to the isochoric specific heat and can be determined from a fit to specific-hear or sound-velocity

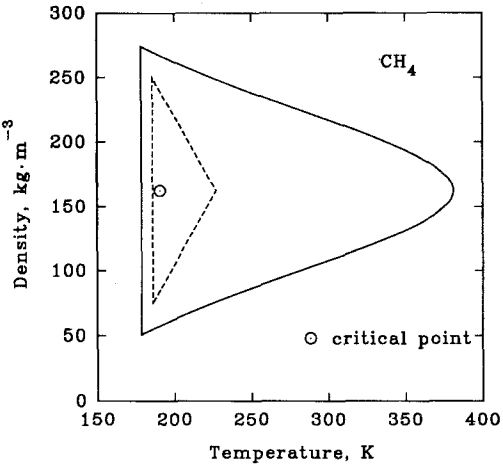

Fig. 2. Range of improved crossover model for methane corresponds to area inside solid curve. Range of crossover model as previously implemented by Jin et al. [36] corresponds to area inside dashed curve.

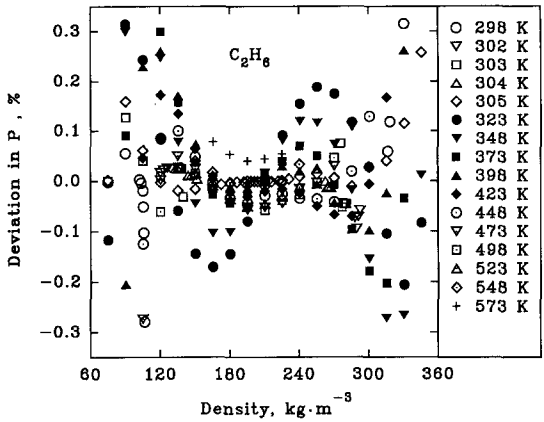

Fig. 3. Percentage deviations of the experimental pressures obtained by Douslin and Harrison [38] for ethane from the values calculated with the crossover model.

data. For ethane we determined the coefficients μ_2 and μ_3 from the c_v data obtained by Shmakov [44] close to the critical point and the coefficient μ_4 from sound-velocity data obtained by Terres et al. [45] and by Tsumura and Straty [46] far away from the critical point. A comparison between the experimental c_v data of Shmakov and the values calculated from the revised crossover model is shown in Fig. 5. The critical temperature implied

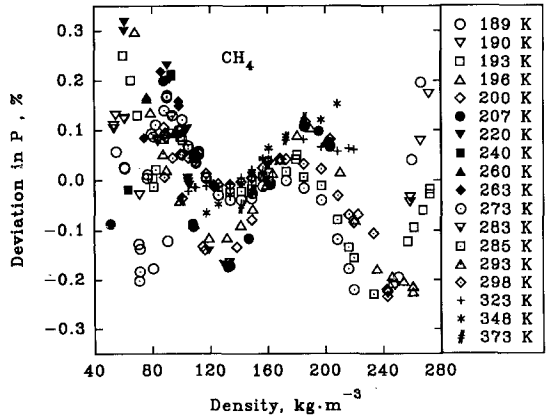

Fig. 4. Percentage deviations of the experimental pressures obtained by Wagner and co-workers [40, 41] and by Trappeniers and co-workers [42] for methane from the values calculated with the crossover model.

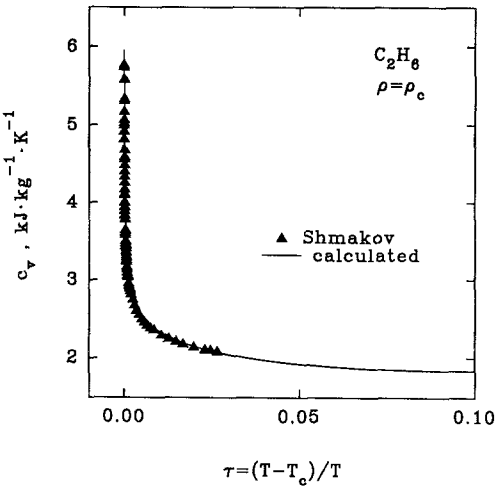

Fig. 5. The isochoric specific heat c_v of ethane along the critical isochore as a function of temperature in the one-hase region above T_c. The symbols indicate experimental data obtained by Shmakov [44] and the solid curve represents values calculated with the cross-over model.

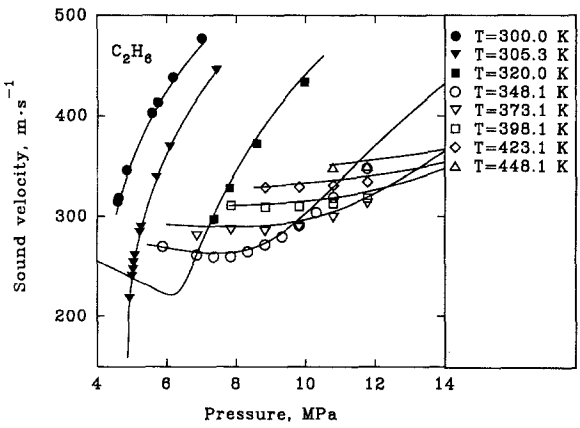

Fig. 6. The sound velocity of ethane at various temperatures in the supercritical region as a function of pressure. The filled symbols indicate experimental data obtained by Tsumura and Straty [46], the open symbols correspond to experimental data obtained by Terres et al. [45], and the curve represents values calculated with the crossover model.

by the c_v data of Shmakov appears to be 0.033 K higher than the value reported by Douslin and Harrison for T_c. When a correction is made for this temperature difference, the c_v data of Shmakov are reproduced with an average deviation of 1.8%, which is within the experimental accuracy. A comparison with experimental sound-velocity data for ethane is shown in Figs. 6 and 7. The crossover model represents the sound-velocity date obtained by Tsumura and Straty [46] with a standard deviation of 1.6% including the near-critical region, where the classical global equation developed by Friend et al. [47] cannot be used. The average deviation of the sound-velocity data obtained by Terres et al. is about 2%. Terras et al. themselves claim an accuracy of only 0.3%, but the deviations found in our analysis are of the same order as those from the equation of Friend et al. [47]. As shown in Fig. 7, there are also some systematic deviations between the sound-velocity data of Terres et al. [45] and those of Tsumura and Straty [46]. A comparison with experimental c_p data of Bier et al. [48] and of Miyazaki et al. [49] is shown in Figs. 8 and 9. At a pressure of 4.473 MPa a small systematic deviation from the experimental data of Miyazaki et al., connected with a difference of the actual locations of the experimental and calculated c_p maxima, is observed.

For methane the coefficients μ_2 and μ_3 were determined from a fit to

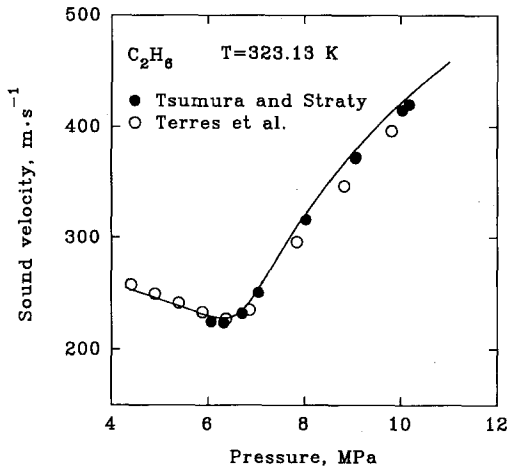

Fig. 7. The sound velocity of ethane as a function of pressure at $T = 323.13$ K. The filled symbols indicate experimental data obtained by Tsumura and Straty [46], the open symbols correspond to experimental data obtained by Terres et al. [45], and the curve represents values calculated with the crossover model.

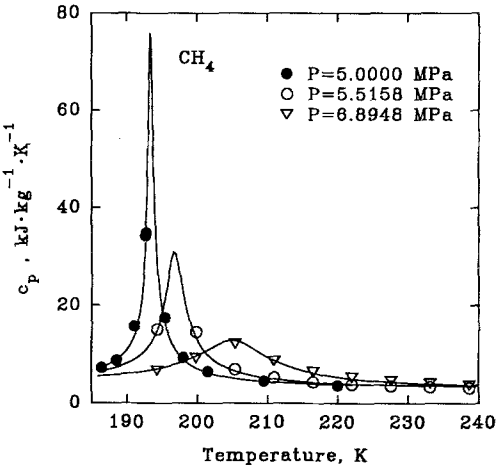

Fig. 8. The isobaric specific heat c_p of ethane at various pressures as a function of temperature. The symbols indicate experimental data obtained by Miyazaki et al. [49] (filled symbols) and by Bier et al. [48] (open symbols) and the curves represent values calculated with the crossover model.

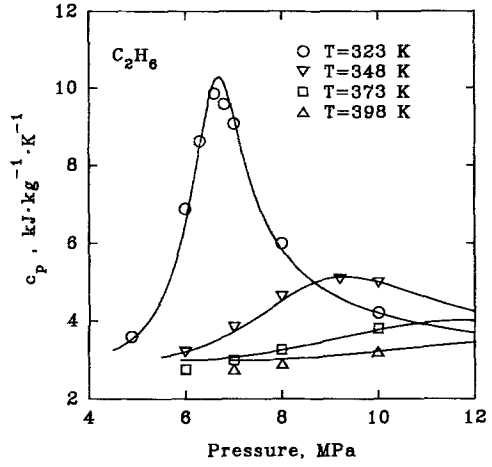

Fig. 9. The isobaric specific heat c_p of ethane at various temperatures as a function of pressure. The symbols indicate the experimental data of Bier et al. [48] and the curves represent the values calculated with the crossover model.

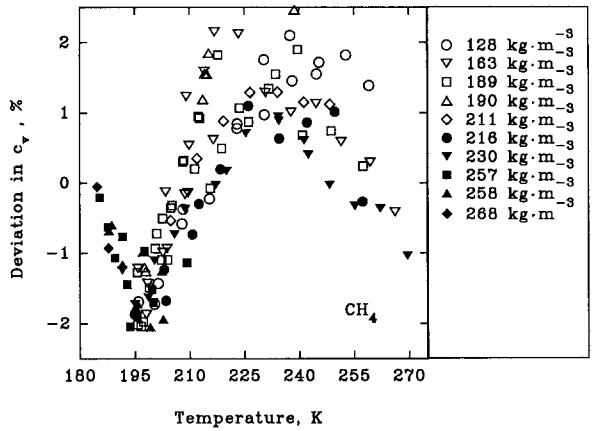

Fig. 10. Percentage deviations of the experimental c_v data [50–52] for methane from the values calculated with the crossover model.

experimental c_v data of Younglove [50], as corrected by Roder [51], and to experimental c_v data obtained by Anisimov et al. [52]. The coefficients μ_4 and μ_5 were determined from a fit to experimental sound-velocity data [53–55]. The critical temperature implied by the c_v data of Anisimov et al., $T_c = 190.678$ K, appears to be 0.114 K higher than the value of T_c obtained by Kleinrahm and Wagner [39] and adopted by us; we shifted the tem-

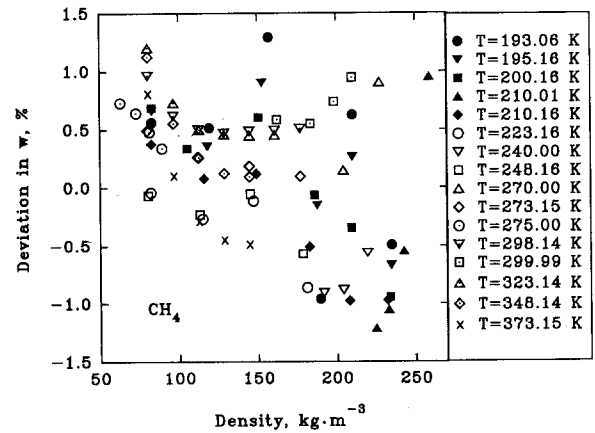

Fig. 11. Percentage deviations of the experimental data for the sound velocity w for methane [53–55] from the values calculated with the crossover model.

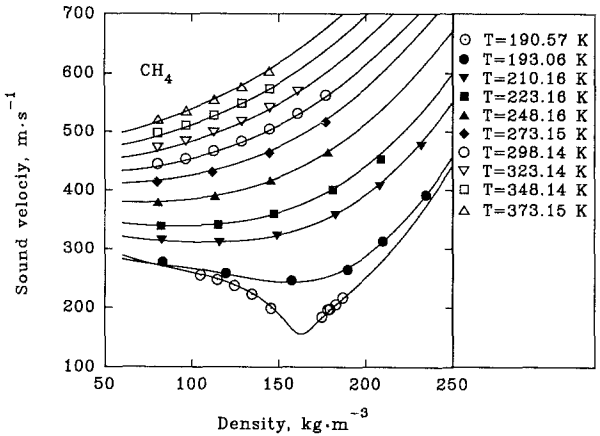

Fig. 12. The sound velocity of methane at various temperatures as a function of density. The symbols indicate experimental data [53–55] and the curves represent values calculated with the crossover model.

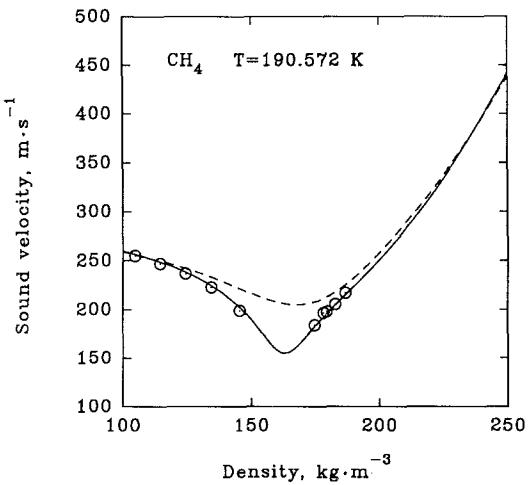

Fig. 13. The sound velocity of methane at $T = 190.572$ K as a function of density. The symbols indicate experimental data obtained by Gammon and Douslin [53], the solid curve represents values calculated with the crossover model, and the dashed curve represents values calculated with the analytic equation of Setzmann and Wagner [43].

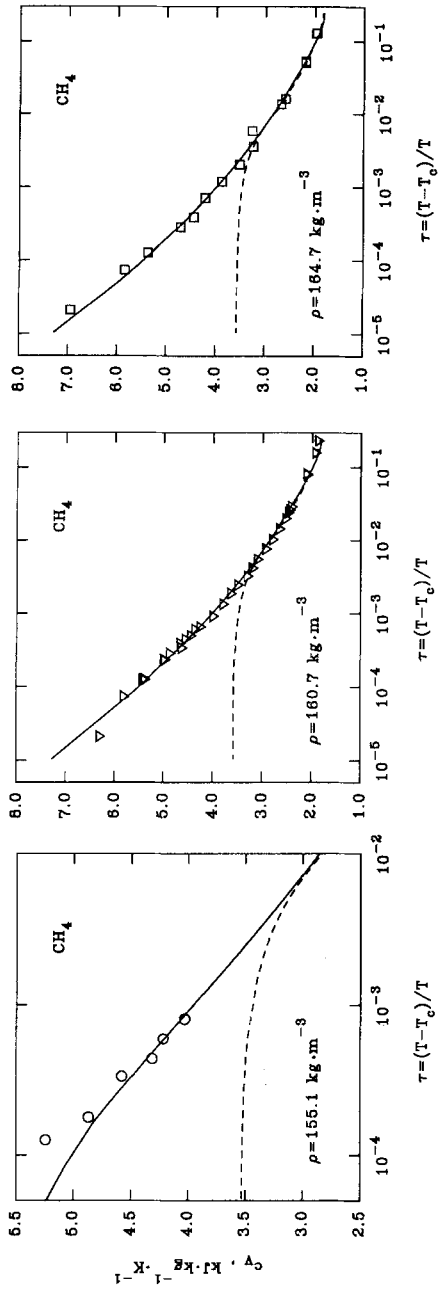

Fig. 14. The isochoric specific heat c_v of methane in the near-vicinity of the critical point. The symbols indicate experimental data obtained by Anisimov et al. [52], the solid curve represents values calculated with the crossover model, and the dashed curve represents values calculated with the analytic equations of Setzmann and Wagner [43].

perature associated with the c_v data of Anisimov et al. by this amount. Deviations of the experimental c_v values from those calculated with the crossover model are shown in Fig. 10. Deviations of the experimental sound-velocity data obtained by Gammon and Douslin [53], Straty [54], and Trusler and Zarari [55] for methane are shown in Fig. 11. The crossover model represents the specific-heat data and the sound-velocity data with a standard deviation of 1.8%, which is within the experimental accuracy. The actual sound-velocity values for methane at various temperatures are plotted as a function of density in Fig. 12. That a good agreement is obtained even at a temperature as high as 373.15 K and at densities that are actually outside the range indicated in Fig. 2.

A comprehensive global analytic equation of state for methane has recently been developed by Setzmann and Wagner [43]. This analytic equation of state yields a very good representation for the thermodynamic properties of methane, but it fails to account for the divergent behavior of the isochoric specific heat at the critical point, which in turn causes the sound velocity to vanish at the critical point. The sound velocity of methane at the near-critical temperature $T = 190.572$ K is shown in Fig. 13. The behavior of our crossover model near the critical point is identical to that of Jin et al. [36], while the analytic equation of Setzmann and Wagner [43] fails to follow the rapid decrease in the sound velocity in the near-vicinity of the critical point. This phenomenon is illustrated even more dramatically in Fig. 14, where a comparison is made with new experimental c_v data obtained by Anisimov et al. [52].

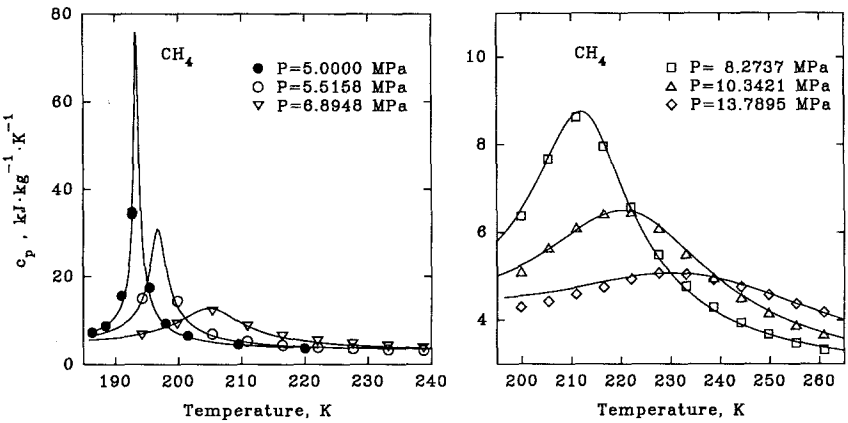

Fig. 15. The isobaric specific heat c_p of methane at various pressures as a function of temperature. The filled symbols indicate experimental data obtained by Kasteren and Zeldenrust [57], the open symbols experimental data obtained by Jones et al. [56], and the curves represent values calculated with the crossover model.

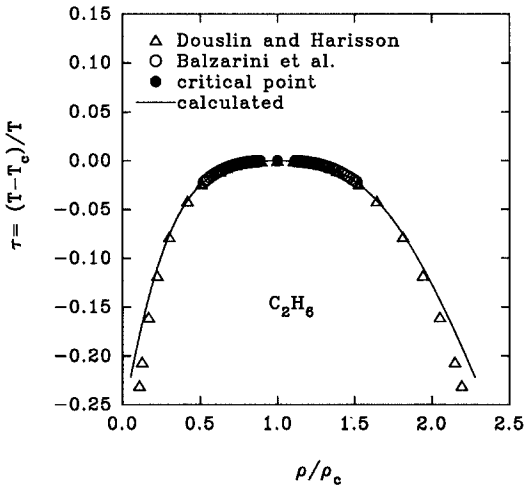

Fig. 16. Densities of the coexisting vapor and liquid phase of ethane as a function of temperature. The symbols indicate experimental data [38, 58–60] and the curve represents values calculated with the crossover model.

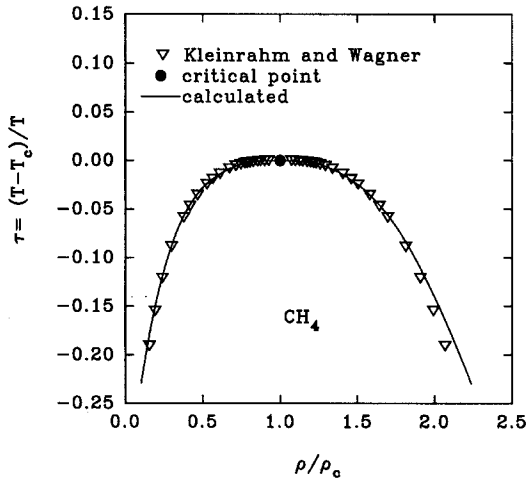

Fig. 17. Densities of the coexisting vapor and liquid phase of methane as a function of temperature. The symbols indicate the experimental data obtained by Kleinrahm and Wagner [39] and the curve represents values calculated with the crossover model.

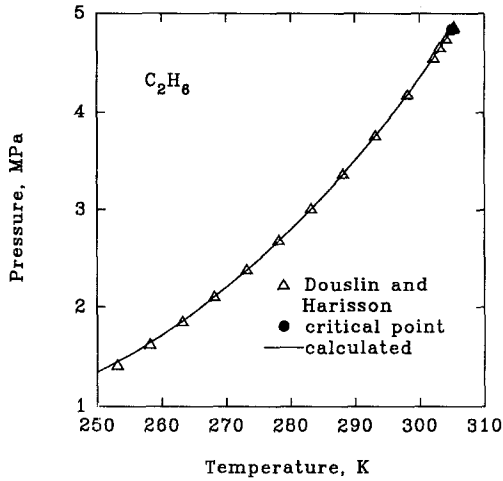

Fig. 18. The vapor pressure of ethane as a function of temperature. The symbols indicate experimental data obtained by Douslin and Harrison [38] and the curve represents values calculated with the crossover model.

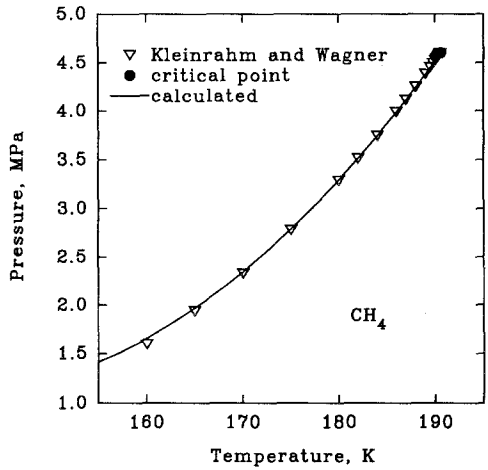

Fig. 19. The vapor pressure of methane as a function of temperature. The symbols indicate experimental data obtained by Kleinrahm and Wagner [39] and the curve represents values calculated with the crossover model.

A comparison with experimental data for the isobaric specific heat of methane is shown in Fig. 15. Good agreement between calculated values and experimental data of Jones et al. [56] and experimental data of Kasteren and Zeldenrust [57] for the isobaric specific heat is observed.

Up to this point we have restricted the analysis of our crossover model to the one-phase region. However, it can also be extrapolated to represent the thermodynamic surface in the two-phase region down to temperatures about 15–20% below the critical temperature. A comparison of our crossover model with experimental vapor and liquid density data is shown in Figs. 16 and 17, and a comparison with vapor-pressure data is shown in Figs. 18 and 19. One problem with scaled equations of state used in the past is that the agreement between experimental and calculated values deteriorated very rapidly as soon as the equations were extrapolated outside their near-critical range of validity. From Figs. 16–19 we see that with a crossover equation of state, the difference between experimental and calculated values increase only gradually upon extrapolation.

6. DISCUSSION

The critical point is a point of marginal thermodynamic stability and the thermodynamic surface of fluids has a singularity at the critical point. This singularity can be characterized by scaling laws with universal exponents and universal scaling functions in the immediate vicinity of the critical point. However, the effects of long-range fluctuations, associated with enhanced values of the compressibility, are not restricted to the immediate vicinity of the critical point but extend over a large range of temperatures and densities around the critical point [16]. To deal with the thermodynamic behavior of fluids in the extended critical region, we have developed an equation of state that includes the crossover from singular behavior near the critical point to regular behavior far away from the critical point. This goal has been accomplished by considering an expansion around the critical point, retaining a finite number of terms and demanding that each term becomes an analytic function for large values of a parametric variable that yields a measure of the distance from the critical point. By comparing this parametric model with experimental thermodynamic-property data, we have demonstrated that such a crossover model can indeed account for the behavior of thermodynamic properties of fluids in a large range of temperatures and densities around the critical point.

APPENDIX I. THE HELMHOLTZ FREE-ENERGY DENSITY IN THE PARAMETRIC FORM

$$\Delta\tilde{A}(r,\vartheta) = kr^{2-\alpha}R^{\alpha}(q)\left[a\Psi_0(\vartheta) + \sum_{i=1}^{5} c_i r^{\Delta_i} R^{-\Delta_i}(q)\,\Psi_i(\vartheta)\right] \tag{A1}$$

$$\tau = r(1-b^2\vartheta^2) \tag{A2}$$

$$m = \Delta\rho - d_1\tau = kR^{-\beta+1/2}(q)\,r^{\beta}\vartheta \tag{A3}$$

The functions $\Psi_0(\vartheta)$ and $\Psi_1(\vartheta)$ are

$$\Psi_0(\vartheta) = (1/2b^4)[2\beta(b^2-1)/(2-\alpha) + 2\beta(2\gamma-1)(1-b^2\vartheta^2)/\gamma(1-\alpha) + (2\beta-1)(1-b^2\vartheta^2)^2/\alpha] \tag{A4}$$

$$\Psi_1(\vartheta) = [1/2b^2(1-\alpha+\Delta_1)][(\gamma+\Delta_1)/(2-\alpha+\Delta_1) - (1-2\beta)\,b^2\vartheta^2] \tag{A5}$$

$$\Psi_2(\vartheta) = [1/2b^2(1-\alpha+\Delta_2)][(\gamma+\Delta_2)/(2-\alpha+\Delta_2) - (1-2\beta)b^2\vartheta^2] \tag{A6}$$

$$\Psi_3(\vartheta) = \vartheta - (2/3)(e-\beta)b^2\vartheta^3 + (1-2\beta)e_1 b^4\vartheta^5/(5-2e) \tag{A7}$$

$$\Psi_4(\vartheta) = (1/3)b^2\vartheta^3 + (1-2\beta)e_2 b^4\vartheta^5/(5-2e) \tag{A8}$$

$$\Psi_5(\vartheta) = (1/3)b^2\vartheta^3 + (1-2\beta)e_4 b^4\vartheta^5/(5-2e_3) \tag{A9}$$

where

$$\Delta_1 = \nu\omega \tag{A10}$$

$$\Delta_2 = 2\Delta_1 \tag{A11}$$

$$\Delta_3 = \Delta_4 = \gamma + \beta - 1 \tag{A12}$$

$$\Delta_5 = \nu\omega_5 \tag{A13}$$

$$b^2 = (\gamma - 2\beta)/\gamma(1-2\beta) \tag{A14}$$

$$e = 2\gamma + 3\beta - 1 \tag{A15}$$

$$e_1 = (5-2e)(e-\beta)(3-2e)/3(5\beta-e) \tag{A16}$$

$$e_2 = (5-2e)(e-3\beta)/3(5\beta-e) \tag{A17}$$

$$e_3 = 2-\alpha+\Delta_5 \tag{A18}$$

$$e_4 = (5-2e_3)(e_3-3\beta)/3(5\beta-e_3) \tag{A19}$$

The crossover function $R(q)$ is

$$R(q) = 1 + q^2/(q_0+q) \tag{A20}$$

with $q = rg$.

APPENDIX II. THE HELMHOLTZ FREE-ENERGY DENSITY IN THE RENORMALIZED FORM

We introduce a new function,

$$\tilde{Y}(q) = [q/R(q)]^{\Delta_1} \tag{A21}$$

and replace the function $R(q)$ in Eqs. (A2) and (A3) by $\tilde{Y}(q)$, so that

$$\vartheta^2 = (m^2/rk^2g^{1-2\beta})\,\tilde{Y}^{(1-2\beta)/\Delta_1} \tag{A22}$$

and

$$r = \tau + (b^2m^2/k^2g^{1-2\beta})\,\tilde{Y}^{(1-2\beta)/\Delta_1} \tag{A23}$$

If we then substitute Eqs. (A22) and (A23) into Eq. (A1) and use the expressions (A4)–(A9) for $\Psi_i(\vartheta)$, we obtain

$$\begin{aligned}\Delta\tilde{A} = {} & (1/2)\,\tilde{a}_{12}\tau m^2\tilde{Y}^{(1-\alpha-2\beta)/\Delta_1} + (1/4!)\,\tilde{a}_{04}m^4\tilde{Y}^{(2-\alpha-4\beta)/\Delta_1} \\ & + (1/5!)\,\tilde{a}_{05}m^5\tilde{Y}^{(2-\alpha-5\beta+\Delta_5)/\Delta_1} + (1/3!)\,\tilde{a}_{13}\tau m^3\tilde{Y}^{(2-\alpha-3\beta+\Delta_5)/\Delta_1} \\ & + (1/2)\,\tilde{a}_{21}\tau^2 m\tilde{Y}^{(1-2\alpha-2\beta)/\Delta_1} - (1/2)\,\tilde{a}_0\tau^2\tilde{Y}^{-\alpha/\Delta_1}\end{aligned} \tag{A24}$$

where the coefficients $\tilde{a}_{ij}$ are given by

$$\begin{aligned}\tilde{a}_{12} = {} & (2a\beta/kb^2g^{1-2\beta-\alpha})\{2(b^2-1)/(2-\alpha) + (2\gamma-1)/\gamma(1-\alpha) \\ & + [c_1b^2/2ag^{\Delta_1}(1-\alpha+\Delta_1)][2(\gamma+\Delta_1)/(2-\alpha+\Delta_1) + (1-2\beta)]\,\tilde{Y} \\ & + [c_2b^2/2ag^{\Delta_2}(1-\alpha+\Delta_2)][2(\gamma+\Delta_2)/(2-\alpha+\Delta_2) + (1-2\beta)]\,\tilde{Y}^2\}\end{aligned} \tag{A25}$$

$$\begin{aligned}\tilde{a}_{04} = {} & [4!\,a\beta(b^2-1)/k^3g^{2-4\beta-\alpha}(2-\alpha)] \\ & \times\{1 + [c_1b^2(2-\alpha)/2ag^{\Delta_1}(1-\alpha+\Delta_1)(b^2-1)] \\ & \times[(\gamma+\Delta_1)/(2-\alpha+\Delta_1) + (1-2\beta)]\,\tilde{Y} \\ & + [c_2b^2(2-\alpha)/2ag^{\Delta_2}(1-\alpha+\Delta_2)(b^2-1)] \\ & \times[(\gamma+\Delta_2)/(2-\alpha+\Delta_2) + (1-2\beta)]\,\tilde{Y}^2\}\end{aligned} \tag{A26}$$

$$\begin{aligned}\tilde{a}_{05} = {} & (5!\,b^4/k^4g^{2-5\beta-\alpha+\Delta_5})\{c_5[1/3 + (1-2\beta)e_4/(5-2e_3)] \\ & + (c^4/g^{\Delta_4-\Delta_5})[1 - 2(e-\beta)/3 + (1-2\beta)e_2/(5-2e)]\,\tilde{Y}^{(\Delta_4-\Delta_5)/\Delta_1} \\ & + (c_3/g^{\Delta_3-\Delta_5})[1 - 2(e-\beta)/3 + (1-2\beta)e_1/(5-2e)]\,\tilde{Y}^{(\Delta_3-\Delta_5)/\Delta_1}\}\end{aligned} \tag{A27}$$

$$\tilde{a}_{13} = (2b^2/k^2 g^{2-3\beta-\alpha+\Delta_5})[c_5 + (c_4/g^{\Delta_4-\Delta_5})\,\tilde{Y}^{(\Delta_4-\Delta_5)/\Delta_1} + (c_3/g^{\Delta_3-\Delta_5})(6+2\beta-2e)\,\tilde{Y}^{(\Delta_3-\Delta_5)/\Delta_1}] \tag{A28}$$

$$\tilde{a}_{21} = 2c_4\, g^{2\beta+2\alpha-1} \tag{A29}$$

$$\tilde{a}_0 = (akg^{\alpha}/b^2)\{\gamma(\gamma-1)/\alpha(1-\alpha)(2-\alpha) - (c_1/ag^{\Delta_1})[(\gamma+\Delta_1)/(1-\alpha+\Delta_1)(2-\alpha+\Delta_1)]\,\tilde{Y} + (c_2/ag^{\Delta_2})[(\gamma+\Delta_2)/(1-\alpha+\Delta_2)(2-\alpha+\Delta_2)]\,\tilde{Y}^2\} \tag{A30}$$

Introducing rescaling functions in analogy to rescaling functions previously introduced by Chen et al. [15],

$$\mathscr{T} = \tilde{Y}^{(2-2\alpha)/\Delta_1} = \tilde{Y}^{(2-1/\nu)/\omega} \tag{A31}$$

$$\mathscr{D} = \tilde{Y}^{(2-\alpha-6\beta)/\Delta_1} = \tilde{Y}^{-\eta/\omega} \tag{A32}$$

$$\mathscr{U} = \tilde{Y}^{(2-\alpha)/3\Delta_1} = \tilde{Y}^{1/\omega} \tag{A33}$$

$$\mathscr{V} = \tilde{Y}^{(2\Delta_5-\nu)/2\Delta_1} = \tilde{Y}^{(\omega_5-1/2)/\omega} \tag{A34}$$

$$\mathscr{V}_1 = \tilde{Y}^{(2\Delta_3-\nu)/2\Delta_1} = \tilde{Y}^{(4-5\alpha-6\beta)/\omega\nu} \tag{A35}$$

$$\mathscr{K} = \tilde{Y}^{-\alpha/\Delta_1} - 1 = \tilde{Y}^{-\alpha/\omega\nu} - 1 \tag{A36}$$

and defining a rescaled order parameter, $M = c_\rho m$, we obtain from Eq. (A24)

$$\Delta\tilde{A} = (1/2)\hat{a}_{12}\tau M^2\mathscr{T}\mathscr{D} + (1/4!)\,\hat{a}_{04}M^4\mathscr{D}^2\mathscr{U} + (1/5!)\,\hat{a}_{05}M^5\mathscr{D}^{5/2}\mathscr{V}\mathscr{U} + (1/3!)\,\hat{a}_{13}\tau M^3\mathscr{T}\mathscr{D}^{3/2}\mathscr{V} + (1/2)\,\hat{a}_{21}\tau^2 M\mathscr{T}^2\mathscr{D}^{1/2}\mathscr{V}_1\mathscr{U}^{-1} - (1/2)\,\hat{a}_0\tau^2\mathscr{K} - (1/2)\,\hat{a}_0\tau^2 \tag{A37}$$

with

$$\begin{aligned} &\hat{a}_{12} = \hat{a}_{12}/c_\rho^2, \quad &&\hat{a}_{04} = \tilde{a}_{04}/c_\rho^2, \quad &&\hat{a}_{05} = \tilde{a}_{05}/c_\rho^5 \\ &\hat{a}_{13} = \tilde{a}_{13}/c_\rho^3, \quad &&\hat{a}_{21} = \tilde{a}_{21}/c_\rho, \quad &&\hat{a}_0 = \tilde{a}_0 \end{aligned} \tag{A38}$$

In the limit $q \gg 1$ ($\tilde{Y} \cong 1$), Eq. (A37) takes the form

$$\Delta\tilde{A} = (1/2)\,a_{12}\tau M^2 + (1/4!)\,a_{04}M^4 + (1/5!)\,a_{05}M^5 + (1/3!)\,a_{13}\tau M^3 + (1/2)\,a_{21}\tau^2 M - (1/2)\,a_0\tau^2 \tag{A39}$$

where the coefficients a_{12}, a_{04}, a_{05}, a_{13}, a_{21}, and a_0 are determined by Eqs. (A25)–(A30) and (A38) with $\tilde{Y} = 1$. The classical theory will be valid as

long as the singular specific heat $A^+\tau^{-\alpha}$ is much smaller than the classical jump $3a_{12}^2/a_{04}$. This condition yields

$$\tau \gg Gi \tag{A40}$$

where the Ginzburg parameter, associated with the specific-heat singularity [16], is

$$Gi \cong g^{-1}[\gamma(\gamma-1)\, b^2(b^2-1)/\beta(2-\alpha)\, \alpha\delta_0^2]^{1/\alpha} \tag{A41}$$

with

$$\delta_0 = 2(b^2-1)/(2-\alpha) + (2\gamma-1)/\gamma(\gamma-1) \tag{A42}$$

ACKNOWLEDGMENTS

The authors are indebted to M. A. Anisimov, G. X. Jin, and J. Luettmer-Strathmann for valuable discussions and assistance. The research of J.V.S. was supported by the Division of Chemical Sciences of the Office of Basic Energy Sciences of the U.S. Department of Energy under Grant DE-F905-88ER13902. The research of S.B.K., as well as travel related to this project, was supported by U.S.-U.S.S.R. Cooperation in the Field of Basic Research of the National Science Foundation under Grant CTS-9022662.

REFERENCES

1. J. V. Sengers and J. M. H. Levelt Sengers, *Annu. Rev. Chem.* **37**:189 (1986).
2. M. A. Anisimov, *Critical Phenomena in Liquids and Liquid Crystals* (Gordon and Breach, Philadelphia, 1991).
3. J. V. Sengers and J. M. H. Levelt Sengers, in *Progress in Liquid Physics*, C. A. Croxton, ed. (Wiley, New York, 1978), p. 103.
4. M. A. Anisimov and S. B. Kiselev, *Sov. Tech. Rev. B Therm. Phys.* **3**(2):1(1992).
5. P. Schofield, J. D. Litster, and J. T. Ho, *Phys. Rev. Lett.* **23**:1098 (1969).
6. J. M. H. Levelt Sengers and J. V. Sengers, in *Perspectives in Statistical Physics*, H. J. Raveché, ed. (North-Holland, Amsterdam, 1981), p. 239.
7. F. W. Balfour, J. V. Sengers, M. R. Moldover, and J. M. H. Levelt Sengers, *Phys. Lett. A* **65**:223 (1978).
8. J. V. Sengers and J. M. H. Levelt Sengers, *Int. J. Thermophys.* **5**:195 (1984).
9. S. B. Kiselev, *High Temp.* **24**:375 (1985).
10. M. A. Anisimov, S. B. Kiselev, and I. G. Kostyukova, *Int. J. Thermophys.* **6**:465 (1985).
11. J. M. H. Levelt Sengers, B. Kamgar-Parsi, F. W. Balfour, and J. V. Sengers, *J. Phys. Chem. Ref. Data* **12**:1 (1983).

12. B. Kamgar-Parsi, J. M. H. Levelt Sengers, and J. V. Sengers, *J. Phys. Chem. Ref. Data* **12**:513 (1983).
13. Kh. S. Abdulkadirova, S. B. Kiselev, I. G. Kostyukova, and L. V. Fedyunina, *J. Eng. Phys.* **61**:902 (1991).
14. A. G. Aizpiri, A. Rey, J. Dávila, R. G. Rubio, J. A. Zollweg, and W. B. Streett, *J. Phys. Chem.* **95**:3351 (1991).
15. Z. Y. Chen, A. Abbaci, S. Tang, and J. V. Sengers, *Phys. Rev. A* **42**:4470 (1990).
16. M. A. Anisimov, S. B. Kiselev, J. V. Sengers, and S. Tang, *Physica A* **188**: 487 (1992).
17. J. Luettmer-Strathmann, S. Tang, and J. V. Sengers, *J. Chem. Phys.* **97**:2705 (1992).
18. J. F. Nicoll, *Phys. Rev. A* **24**:2203 (1981).
19. P. C. Albright, J. V. Sengers, J. F. Nicoll, and M. Ley-Koo, *Int. J. Thermophys.* **7**:75 (1986).
20. Z. Y. Chen, P. C. Albright, and J. V. Sengers, *Phys. Rev. A* **41**:3161 (1990).
21. S. B. Kiselev, *High Temp.* **28**:42 (1988).
22. S. B. Kiselev, I. G. Kostyukova, and A. A. Povodyrev, *Int. J. Thermophys.* **12**:877 (1991).
23. F. J. Wegner, *Phys. Rev. B* **5**:4529 (1972).
24. M. Ley-Koo and M. S. Green, *Phys. Rev. B* **23**:3650 (1981).
25. A. J. Liu and M. E. Fisher, *Physica A* **156**:35 (1989).
26. S. Tang, J. V. Sengers, and Z. Y. Chen, *Physica A* **179**:344 (1991).
27. D. S. Kurumov and B. A. Grigoryev, *Int. J. Thermophys.* **12**:549 (1991).
28. D. J. Wallance and R. K. P. Zia, *J. Phys. C* **7**: 3480 (1974).
29. A. T. Berestov, *Sov. Phys. JETP* **45**:184 (1977).
30. J. Souletie, H. Martin, and C. Tsallis, *Europhys. Lett.* **2**:2360 (1981).
31. E. Carré and J. Souletie, *J. Magnet. Magnet Mater.* **72**:29 (1988).
32. F. C. Zhang and R. K. P. Zia, *J. Phys. A* **15**:3303 (1982).
33. K. E. Neuman and E. K. Riedel, *Phys. Rev. B* **30**:6615 (1984).
34. F. C. Zhang, Ph.D. thesis (Department of Physics, Virginia Polytechnic Institute, Blacksburg, 1983).
35. G. X. Jin, S. Tang, and J. V. Sengers, in press.
36. G. X. Jin, S. Tang, and J. V. Sengers, *Int. J. Thermophys.* **13**:671 (1992).
37. H. Preston-Thomas, *Metrologia* **27**:3 (1992).
38. D. R. Douslin and R. H. Harrison, *J. Chem. Thermodynam.* **5**:491 (1973).
39. R. Kleinrahm and W. Wagner, *J. Chem. Thermodynam.* **18**:739 (1986).
40. R. Kleinrahm, W. Duschek, and W. Wagner, *J. Chem. Thermodynam.* **18**:1103 (1986).
41. G. Händel, R. Kleinrahm, and W. Wagner, *J. Chem. Thermodynam.* **24**:685 (1992).
42. N. J. Trappeniers, T. Wassenaar, and J. C. Abels, *Physica A* **98**:289 (1979); Erratum, Physica A **100**:660 (1980).
43. U. Setzmann and W. Wagner, *J. Phys. Chem. Ref. Data* **20**:1061 (1991).
44. N. G. Shmakov, *Teplofiz. Svoistva Verhchestv Mater. (USSR)* **7**:155 (1973).
45. V. E. Terres, W. Jahn, and H. Reissmann, *Brennstoff-Chemie* **38**:129 (1957).
46. R. Tsumura and G. C. Straty, *Cryogenics* **17**:195 (1977).
47. D. G. Friend, J. F. Ely, and H. Ingham, *J. Phys. Chem. Ref. Data* **18**:583 (1989).
48. K. Bier, J. Kunze, and G. Maurer, *J. Chem. Thermodynam.* **8**:857 (1976).
49. T. Miyazaki, A. V. Hejmadi, and J. E. Powers, *J. Chem. Thermodynam.* **12**:105 (1980).
50. B. A. Younglove, *J. Res. Natl. Bur. Stand. (USA)* **78A**:401 (1974).
51. H. M. Roder, *J. Res. Natl. Bur. Stand. (USA)* **80A**:739 (1976).
52. M. A. Anisimov, V. G. Beketov, V. P. Voronov, V. B. Nagaev, and V. A. Smirnov, *Teplofiz. Svoistva Veshchestv Mater. (USSR)* **16**:124 (1984).
53. B. E. Gammon and D. R. Douslin, *J. Chem. Phys.* **64**:203 (1976).
54. G. C. Straty, *Cryogenics* **14**:367 (1974).

55. J. P. M. Trusler and M. Zarari, *J. Chem. Thermodynam.* **24**:973 (1992).
56. M. L. Jones, D. T. Mage, R. C. Faulkner, and D. L. Katz, *Chem. Eng. Progr. Symp. Ser.* **59**:52 (1963).
57. P. H. G. van Kasteren and H. Zeldenrust, *Ind. Eng. Chem. Fundam.* **18**:333 (1979).
58. M. Burton and D. Balzarini, *Can. J. Phys.* **52**:2011 (1974).
59. D. Balzarini and M. Burton, *Can. J. Phys.* **57**:1516 (1979).
60. M. W. Pestak, R. E. Goldstein, M. H. W., Chan, J. R. de Bruyn, D. A. Balzarini, and N. W. Ashcroft, *Phys. Rev. B* **36**:599 (1987).